Monitoring Myocardial Edema Tissue With Electrical Impedance Spectroscopy

Nazanin Neshatvar[1], Louis Regnacq[2], Dai Jiang[1], Yu Wu[1], and Andreas Demosthenous[1]

[1]Department of Electronic and Electrical Engineering, University College London, Torrington Place, London WC1E 7JE, UK
[2]ETIS UMR8051, CY University, ENSEA, CNRS, F-95000, Cergy, France
Email: n.neshatvar@ucl.ac.uk

***Abstract*— A new approach for monitoring myocardium edema is introduced. It utilizes electrical impedance spectroscopy (EIS) to characterize edema tissue. The system has been tested on an isolated pig heart to distinguish the edema from non-edema tissue by a decrease of impedance for edema. The impedance reduction for left ventricular was 10 Ω at 100 kHz. The algorithm used for the demodulation in the developed EIS system is based on Goertzel filter which is utilized to replace the traditional coherent demodulation technique. Multisine excitation with 16 tones in the frequency range up to 1 MHz with more than 1000 samples was used for the measurements.**

Keywords*— Edema, electrical impedance spectroscopy (EIS), multisine excitation, myocardial.

I. Introduction

Myocardial infarction (MI) is a major cardiac disease that is the consequence of the complete occlusion of the coronary arteries which supply oxygen-rich blood to the myocardium [1]. Followed by MI, myocardial water content is retained within the myocardial tissue and causes swelling in the affected area of myocardial. This is known as edema. Edema has a significant impact on left ventricle (LV) function [2]. Myocardial edema affects cardiac function in a variety of pathologic states. It has been associated with reperfusion injury after acute myocardial ischemia, acute cellular rejection in cardiac transplants, an increase in left ventricular stiffness and impairment of diastolic filling [3]. In addition, myocardial edema decreases cardiac output and, when chronic, can cause interstitial fibrosis [4]. Acute myocardial edema is associated with increased stiffness of papillary muscle and impairment of left ventricular systolic and diastolic function, including decreased left ventricular chamber compliance [5]. Therefore, it is of prime concern to distinguish edema tissue for prognosis purposes.

As a non-invasive diagnostic tool cardiac magnetic resonance (CMR) allows accurate tissue characterization of the myocardium. In particular, T2-weighted (T2W) and T2-mapping CMR sequences have the potential to identify tissues with high water content [6]. Tissue with high water content will appear bright on T2 weighted images, because of the stronger signal intensity feedback from protons within water molecules which shows a close correlation between T2 and edema in the heart [4]. T2-mapping may allow for a more sensitive and objective detection of changes in myocardial water content by means of altered T2 relaxation.

Nevertheless, they both suffer from well-known limitations. In T2W techniques, there is a need for a normal reference region of interest in remote myocardium which can lead to false-negative results when these reference areas are also affected by systemic processes. T2-mapping techniques based on dark-blood turbo spin echo sequences are sensitive to ghosting and motion artefacts. They also exhibit heart-rate dependency, sensitivity to the order of acquisition, and errors in the T2 relaxation time measurements [7]. These can lead to potential difficulties in discriminating between health and disease. While T2 is an inherent tissue property, a recent study in healthy volunteers demonstrated that myocardial T2 varies significantly [7].

Manual contouring is used to quantify the edema size. This is usually performed by an expert clinician. The presence of signal void due to myocardium haemorrhage and the weak edge information on epicardium boundary are two major challenges which need to be addressed [1]. Although this area of signal void is usually included in the edema area by the clinician, the difficulty is that the area has different tissue characteristic compared to the edema. Several semiautomatic contouring methods including standard deviation (SD) method have been introduced to facilitate the quantification of edema. These quantification methods required the user to select normal region or edema region for setting up the threshold value [1]. Considering a fully automatic method where the threshold is automatically set based on image intensity information and the use of feature analysis to eliminate spurious small positive bright objects on the LV wall and to compensate dark areas of signal void, will improve the result [1][8]. Nonetheless, the images are still based on T2 which can vary and risk the results.

Accurately defining the myocardium from cardiac T2 and delayed enhanced (DE) MRI is a prerequisite for identifying and quantifying the edema and infarcts [8]. The automatic delineation is, however, challenging due to the heterogeneous intensity distribution of the myocardium. Two reasons that result in this complexity are: first, the boundary between the interface and blood pools is

This work was funded by the European Commission under H2020-EU.1.2.2. – FET Proactive (Agreement ID: 824071).

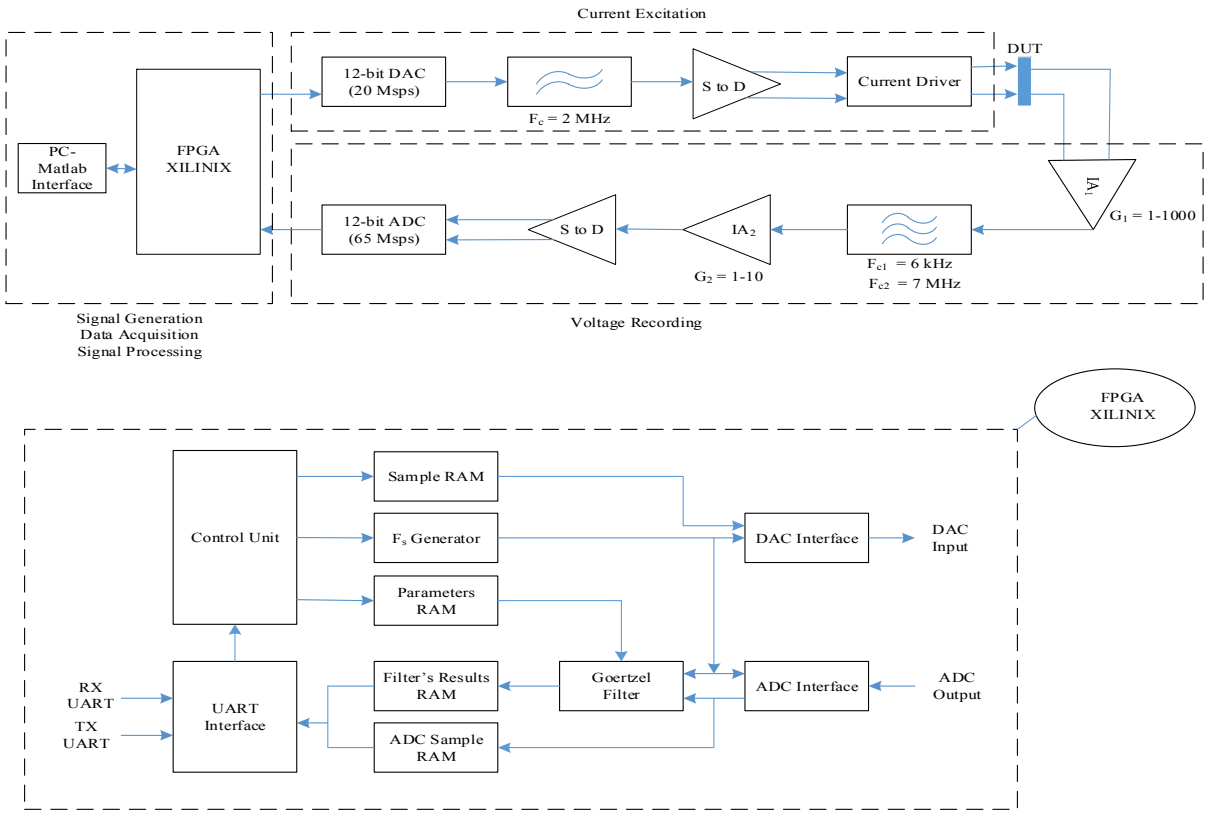

Fig. 1. Block diagram of the EIS system used for characterizing edema impedance. Top part represents AFE and FPGA; lower part represents subsections of the FPGA.

generally indistinct and particularly difficult to delineate and second , the intensity of the myocardium is not normally distributed in either the T2 or DE sequence [8].

As an alternative approach for characterising the edema tissue, impedance measurement can be done via tetra-polar electrical impedance spectroscopy (EIS). In tetra-polar EIS a sinusoidal current is applied to a pair of electrodes and the voltage is measured via the other pair. In this configuration, the electrode/tissue interface is minimized. The current voltage relationship provides an estimation of the impedance of the tissue under study over the frequency range of interest. As a measurement tool, EIS can be utilized to differentiate the edema tissue. For a maximized edema tissue the water content is high which translates to low impedance.

This paper presents a different method to previous techniques by using impedance measurements and Goertzel filtering for characterizing edema tissue. Section II discusses the system level design of the proposed EIS system. Section III shows measurement results using the EIS system for both a resistive/capacitive (RC) load and an isolated pig heart. Section IV summarizes the work and provides an outlook to future work.

II. EIS System Level Architecture

The EIS system utilizes a broadband signal to allow impedance evaluation at several frequencies with a single measurement. Considering hardware constraints, a low crest factor improves quantization noise and consequently the measurement precision. For tuneable spectral distribution where the energy must be contained in the measurement bandwidth, a multitone signal can provide three degrees of freedom represented by amplitude, frequency and phase of each tone. The generated multi-sine excitation signal for the EIS system is composed of 16 sinewaves between 10 kHz and 1 MHz with a total of 1000 samples and a sampling frequency of 5 Msps to cover alpha and beta dispersion regions. By tuning the relative phases of each of the tones, a low crest factor can be obtained.

The multi-sine EIS system mainly comprises two parts: an analog front-end (AFE) and a field programmable gate array (FPGA). The overall system is controlled from a computer with Matlab interface. A block diagram of the system is shown in Fig. 1. The AFE includes current excitation and voltage measurements. A 12-bit digital-to-analog converter (DAC) provides the necessary input for the current driver. The DAC is clocked via the FPGA and followed by an anti-aliasing filter. A single-to-differential amplifier (S to D) generates the differential input to the current driver which in turn produces constant current amplitudes to drive the load (DUT). The induced voltage is first amplified by a programmable gain instrumentation amplifier (PGA) with a digitally programmable gain between 1 and 1000 V/V. The output is band pass filtered and amplified by a second PGA with a programmable gain of 1-10 V/V to extend the voltage sensing capabilities. The output of the second PGA is digitized by a 12-bit ADC at 65 Msps. The overall bandwidth of the system is defined by the bandpass filter's cut-off frequencies from 6 kHz to 7 MHz.

In the FPGA architecture, the control unit receives, decodes and executes the instruction from the PC via

TABLE I
SYSTEM PERFORMANCE CHARACTERISTICS

Parameter	Value
Current amplitude	50 μA_{p-p}
No. of sinewaves (tones)	16
Frequency range	10k Hz to 1 MHz
Centre frequency	100 kHz
Sampling frequency	5 Msps
No. of samples	1000
Measurement duration	300 µs (100 µs for settling)
Sampling frequency (DAC)	Up to 20 Msps
Sampling frequency (ADC)	Up to 65 Msps

UART interface where the instruction can either be stored as parameters inside the FPGA RAM, or used to trigger the measurement. A detailed view of FPGA analysis is shown in Fig. 1 (bottom section).

Once triggered from the UART interface, the FPGA drives the DAC with desired low crest factor multi-sine. The induced voltage in the load is sensed and digitized. The samples can be either stored and sent to the computer for offline processing, or be demodulated inside the FPGA. The algorithm used for demodulation is based on the Goertzel filter [9], which is used to replace the traditional coherent demodulation (IQ demodulation) technique. It can be explained by converting the discrete time Fourier transform (DTFT) equation into a recursive filter:

$$X(m) = \sum_{n=0}^{N-1} x(n) e^{-\frac{2j\pi mn}{N}} \quad (1)$$

$$X(m) = (((W_N^m x(0) + x(1))\, W_N^m + x(2))W_N^m + \cdots + x(N-1))W_N^m \quad (2)$$

$$W_N^m = e^{\frac{-2j\pi mn}{N}} \quad (3)$$

The filter can be realized with a second-order IIR structure and split in two parts: a recursive part with one real multiplication, and a feedforward path using one complex multiplication. The complex feedforward path itself can be split into two real paths, requiring two real multiplications. The recursive part is performed N times (with $x(N) = 0$ at time $n = N$, where $x(N)$ is the input), whereas the feedforward is performed only once, for $W(N)$ [10]. Therefore, the total number of multiplications is $N + 2$ and the total number of additions is $2N + 1$ additions. This leads to only three coefficients being stored: one for the recursive part and two for the feed-forward part (real and imaginary part).

This filter performs the computation of the Fourier coefficients at the same time as the sampling occurs. Therefore, in contrast to the conventional fast Fourier transform computation, no sample storage is needed, and no delay is added. Furthermore, unlike IQ demodulation this filter does not require to store a full sine/cosine cycle as the reference signal, but only 3 coefficients per bin. Since it is resonating around the bin of interest, it does not suffer from harmonic fold back, therefore does not require a high sampling frequency.

By using a defined resistive load, the measurement is triggered, and calibration coefficients are computed. A summary of the overall system performance is provided in Table. I.

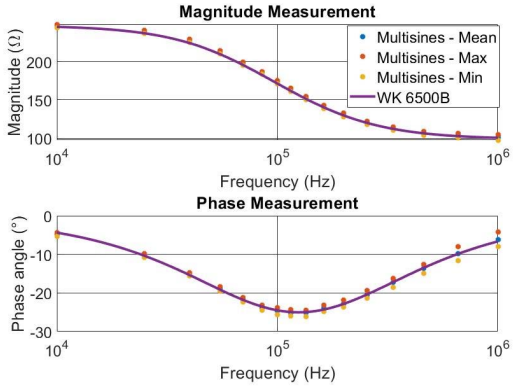

(a)

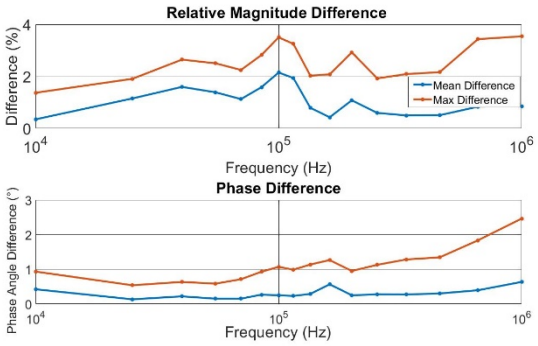

(b)

Fig. 2. (a) Measurement comparison of magnitude difference and phase difference of the multi-sine EIS system and a commercial impedance analyser (Wayne Kerr 6500B) (b) Mean and maximum difference for magnitude and phase measurements.

III. Measurement Results

A. EIS System Performance

The multi-sine EIS system was first tested with an RC load comprising a parallel combination of (150Ω || 15nF) in series with 100 Ω resistor. The load presents an inflexion point around 100 kHz. Therefore, a bilateral quasi log (BQL) distribution composed of 16 tones, from 10 kHz to 1 MHz, centred around 100 kHz is generated. The signal's length is three cycles of the lowest frequency; with a duration of 300 μs. The measurement is realized over 2 cycles, keeping the first one for settling. With a sampling frequency of 5 Msps, the measurement results in over 900 samples. To compare the accuracy, the load was measured with a Wayne Kerr 6500B impedance analyser over the same frequency range. The result for magnitude and phase is shown in Fig. 2(a). The maximum difference on the magnitude is about 5 Ω (2.5 %) and 1° (4 %) on the phase. Non-linear least mean square algorithm was used to fit the data in order to estimate the value of the two resistors and the capacitor. The mean and maximum difference for the frequency range of 10 kHz to 1 MHz is shown in Fig. 2(b).

B. Impedance Measuremnt of Edema Myocardium in Isolated Pig Heart

An ex-vivo impedance measurement on an isolated pig heart using the multi-sine EIS system was performed at different locations and three electrode positions. The results were compared to the impedance measurement from Wayne Kerr at the same electrode positions as a reference

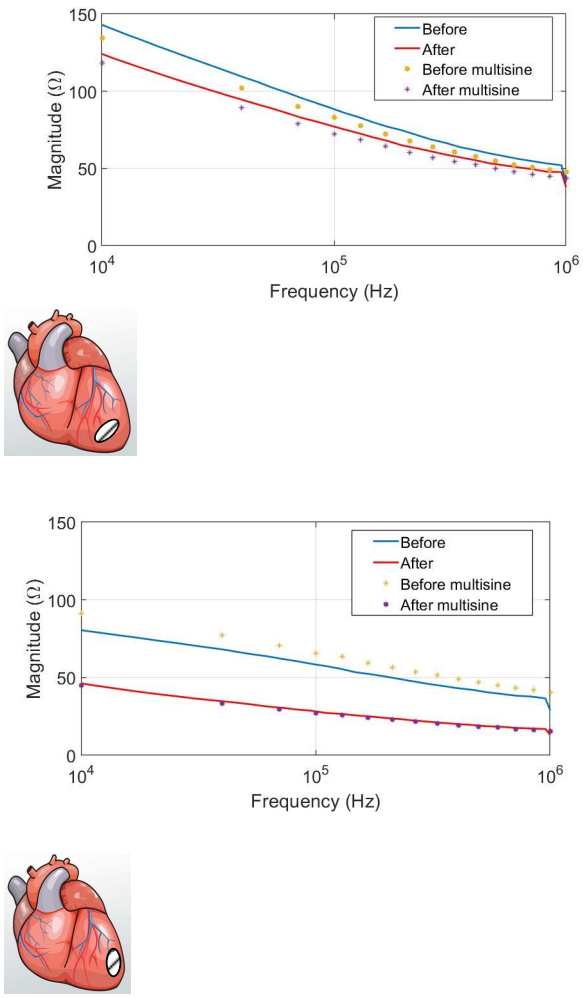

Fig. 3. Impedance magnitude of the isolated pig heart before (blue) and after (red) soaked in PBS at different electrode positions of the heart, the four electrodes are assumed to be placed the in white box.

for accuracy. The four in-line electrodes used were Myocardial-Lead TME 67T from Osypka. The spacing between each electrode was 4 mm. In the tetrapolar configuration the outer electrodes were used for current injection and the two inner electrodes were used for voltage measurements. The drive current was 50 $\mu_{Ap\text{-}p}$.

The multi-sine measurement showed good accuracy and was able to detect small changes in the impedance measurement. In order to estimate whether the tissue is oedema or not, the pig heart was soaked in phosphate-buffered saline (PBS) solution for one hour and then the impedance measurements were taken. The electrodes were placed at different positions on the LV so that the effect of myocardium oedema after MI can be suitably analysed. These electrodes were fixed in position for the Wayne Kerr and multi-sine tests. These results were compared with the impedance before soaking. The results in Fig. 3 show the impedance magnitude of the heart tissue at two different electrode positions before and after being soaked in PBS. They show an impedance shift (lower impedance) which represents absorption of the fluid by tissue and can be characterized as edema. This change varies in different electrode positions. For a diagonal position on the LV it is 10 Ω at 100 kHz whereas for a more vertical position this difference is about 30 Ω at 100 kHz Although the system provides accurate measurements for RC loads when compared to Wayne Kerr impedance analyser, this was not the case for ex-vivo measurements. This can be attributed to the position of the electrodes and their arrangements. Further investigation is under study.

IV. Conclusion

A new method to characterize edema tissue based on EIS has been proposed and was successfully tested on an isolated pig heart. It shows that the impedance of the edema tissue is lower than a healthy one due to the presence of water. The multi-sine EIS system is based on Goertzel algorithm and has been successfully used to replace the traditional coherent demodulation (IQ demodulation) technique. Further investigations will perform the measurements over a longer period to examine the variation of magnitude and phase of the impedance with time.

References

[1] K. Kadir, A. Payne, J. J. Soraghan, and C. Berry, "Automatic quantification of oedema from T2 weighted CMR image using a Hybrid Thresholding Oedema Sizing Algorithm (HTOSA)," *Comput. Cardiol. (2010).*, vol. 37, pp. 233–236, 2010.

[2] K. Kadir, H. Gao, A. R. Payne, J. Soraghan, and C. Berry, "Two statistical mixture model vs. fuzzy C-means: In the application of edema segmentation," *IEEE ICSIPA 2013 - IEEE Int. Conf. Signal Image Process. Appl.*, no. i, pp. 333–336, 2013.

[3] C. L. Dent, M. J. Scott, S. A. Wickline, and C. S. Hall, "Monitoring of myocardial edema with quantitative ultrasonic parametric imaging," *Proc. IEEE Ultrason. Symp.*, vol. 2, pp. 1329–1332, 1999.

[4] M. G. Friedrich, "Myocardial edemaa new clinical entity?," *Nat. Rev. Cardiol.*, vol. 7, no. 5, pp. 292–296, 2010.

[5] K. V. Desai *et al.*, "Mechanics of the left ventricular myocardial interstitium: Effects of acute and chronic myocardial edema," *Am. J. Physiol. - Hear. Circ. Physiol.*, vol. 294, no. 6, pp. 2428–2434, 2008.

[6] R. Fernández-Jiménez *et al.*, "Myocardial edema after ischemia/reperfusion is not stable and follows a bimodal pattern: Imaging and histological tissue characterization," *J. Am. Coll. Cardiol.*, vol. 65, no. 4, pp. 315–323, 2015.

[7] V. M. Ferreira, S. K. Piechnik, M. D. Robson, S. Neubauer, and T. D. Karamitsos, "Myocardial Tissue Characterization by Magnetic," vol. 29, no. 3, pp. 147–154, 2014.

[8] J. Liu *et al.*, "Myocardium segmentation combining T2 and DE MRI using multi-component bivariate Gaussian mixture model," *2014 IEEE 11th Int. Symp. Biomed. Imaging, ISBI 2014*, pp. 886–889, 2014.

[9] P. Sysel and P. Rajmic, "Goertzel algorithm generalized to non-integer multiples of fundamental frequency," *EURASIP J. Adv. Signal Process.*, vol. 2012, no. 1, pp. 1–8, 2012.

[10] D. L. Jones, *Digital Signal Processing: A User's Guide*. 2008.